

Hawthorneite, Ba[Ti₃Cr₄Fe₄Mg]O₁₉: A new metasomatic magnetoplumbite-type mineral from the upper mantle

STEPHEN E. HAGGERTY

Department of Geology, University of Massachusetts, Amherst, Massachusetts 01003, U.S.A.

IAN E. GREY, IAN C. MADSEN

Division of Mineral Products, CSIRO, Box 124, Port Melbourne, Victoria 3207, Australia

A. J. CRIDDLE, C. J. STANLEY

Department of Mineralogy, British Museum (Natural History), Cromwell Road, London SW7 5BD, England

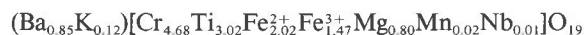
A. J. ERLANK

Department of Geochemistry, University of Cape Town, Rondebosch, 7700, South Africa

ABSTRACT

A new opaque mineral oxide is described from a veined, metasomatized, harzburgitic xenolith from a diamondiferous kimberlite pipe in Kimberley, South Africa. The new mineral, hawthorneite (~100 μm in maximum dimension), is in intimate association with lindsleyite (Ba,Sr)(Ti,Cr...)₂₁O₃₈, a member of the crichtonite group, accessory niobian chromian rutile, and magnesian chromian ilmenite in host-replacement-textured magnesian chromite.

Hawthorneite is isostructural with magnetoplumbite Pb(Fe,Mn)₁₂O₁₉ and barium ferrite (BaFe₁₂O₁₉). Typical electron-microbeam analyses of hawthorneite give TiO₂ = 22.2–23.6, Cr₂O₃ = 33–34.9, FeO = 23.3–24.9, BaO = 12–13, and MgO = 2.9–3.5, with K₂O, ZrO₂, Al₂O₃, MnO, and Nb₂O₅ in the range 0.1–0.5 (all wt%). A typical average composition is



or ideally Ba[Cr₄Ti₃Fe₄Mg]₂₁₂O₁₉.

The space group is *P*6₃/*mmc* with *Z* = 2, and the strongest reflections are [*d*_{calc}(Å), *I*_{calc}, *hkl*] 2.616(100)(114), 2.765(85)(017), and 2.414 (49)(023). Hexagonal unit-cell parameters are *a* = 5.871(2) Å and *c* = 23.06(2) Å, and the structure comprises alternating spinel-type slabs and perovskite-type layers. The calculated density is 5.02 g/cm³.

Hawthorneite is pale gray in reflected light, is nonpleochroic with weak to moderate bireflectance, and has weak to moderate rotation tints in browns and grays. Quantitative spectral reflectance measurements for *R*_o and *R*'_o in air and oil immersion, respectively, are for 470 nm 18.3, 17.1 and 6.02, 5.25%; for 546 nm 17.5, 16.4 and 5.58, 4.88%; for 589 nm 17.3, 16.3 and 5.41, 4.75%; and for 650 nm 17.05, 16.0 and 5.34, 4.68%. VHN₁₀₀ = 801, with a range of five indentations = 772–835.

Hawthorneite is interpreted to have formed by reaction of a Ba-, K-, Ti-, Zr-, and Nb-enriched fluid or volatile-rich melt with magnesian chromite in previously depleted harzburgite. An orientation relationship between spinel and hawthorneite is preserved such that [111]_{Sp}||[0001]_{Haw} and (22 $\bar{4}$)_{Sp}|| (30 $\bar{3}$ 0)_{Haw} and in which (Ba + Ti) in fluid replaces (Mg + Cr) in spinel. Continued reaction yields lindsleyite. Conditions of formation are estimated at 900–1100 °C and 20–30 kbar.

Hawthorneite is the Ba analogue of K-characteristic yimengite (K(Cr,Ti...)₁₂O₁₉), which coexists with K-specific mathiasite of the crichtonite group. By contrast, the assemblage hawthorneite + lindsleyite is Ba specific. The small (M) cations in these minerals and in yimengite + mathiasite are Ti + Cr, with lesser Fe, Mg, Zr, and Nb. The similarities in these magnetoplumbite and crichtonite isotypes, and in the associated silicates and oxides, demonstrate a *P-T* crystallochemical underpinning that results from similarities in metasomatic fluids or melts, enrichment processes, and host rocks in widely separated subcontinental subcratonic Archean lithospheres.

The mineral is named for John Barry Hawthorne in honor of his contributions to upper-mantle studies.

INTRODUCTION

Lindsleyite and mathiasite have been described as new minerals in metasomatized peridotite xenoliths from four kimberlites in South Africa (Haggerty et al., 1983). These minerals are members of the crichtonite group, which has the general formula $AM_{21}O_{38}$, where the large A cation is Sr in crichtonite, Na in landauite, Pb in senaite, Ca in loweringite, and REEs in davidite and where the small M cations are dominantly Ti but also Cr, Mg, Fe, Mn, Zn, Zr, and Nb (Grey et al., 1976; Grey and Lloyd, 1976; Gatehouse et al., 1978; Grey and Gatehouse, 1978). Lindsleyite is Ba specific and mathiasite is K characteristic in the large cation site. Mathiasite has since been recognized in kimberlites from the Shandong Province in China (Zhou et al., 1984), in association with another new oxide mineral named yimengite (Dong et al., 1983). Yimengite, in common with mathiasite, is K-specific but with the generalized formula $AM_{12}O_{19}$, where A = large cation and M = the same small cations present in the crichtonite group. The site is again dominated by Ti, but Cr is also present in substantial concentrations, a feature shared with lindsleyite and mathiasite.

In our continuing study of upper-mantle metasomites, it has been assumed that Cr is a restite element in depleted harzburgites and that Ti is introduced metasomatically from deeper regions of the upper mantle to form these exotic high-temperature and high-pressure large-cation (K, Ba) chromian titanates (Haggerty, 1983, 1987; Erlank et al., 1987). That assumption is indeed confirmed, because we now recognize that chromian spinel on reaction with upper-mantle fluids or melts proceeds to form lindsleyite or mathiasite ($AM_{21}O_{38}$), depending on whether the metasomatizing agent is enriched in Ba or K, but does so via an intermediate and nonequilibrium reaction in which an $AM_{12}O_{19}$ phase is formed (Haggerty et al., 1986). In K-rich upper-mantle metasomatic environments, the $AM_{12}O_{19}$ mineral is yimengite. Since the associated crichtonite-group mineral is mathiasite (K), the Ba member of the $AM_{12}O_{19}$ group is predicted to coexist with lindsleyite and is described here as the new mineral hawthorneite.

Hawthorneite is named for John Barry Hawthorne, Anglo American Corporation, formerly Chief Geologist (Diamonds), De Beers Consolidated Mines, Republic of South Africa, in recognition of his foundation studies on carbonatitic kimberlites and his classic formulation and model of kimberlite pipes. In particular, he is recognized for fostering an unprecedented relationship between industry and fundamental research in academia by initiating studies on, and distributing xenoliths and kimberlites from diamondiferous and nondiamondiferous pipes throughout southern Africa to the international scientific community. This liaison has increased our knowledge and accelerated our understanding of the Kaapvaal craton, so widely used as a model for upper-mantle petrogenetic processes. Hawthorneite has been approved by the International Mineralogical Association, Commission on New

Minerals and New Mineral Names. Type material is deposited at the British Museum (Natural History), London, as BM 1988,71.

SAMPLE LOCATION AND DESCRIPTION

Hawthorneite has thus far been identified in only one sample from the Bultfontein mine (Boshof Road waste dumps) in Kimberley, South Africa. This sample, BD3096, is a complexly veined, metasomatized, harzburgitic xenolith that is dominated by a substrate of coarse (~5 mm) olivine and enstatite, subordinate 1- to 3-mm laths of phlogopite, and lesser potassian richterite. Veins, 1–5 mm in width and crosscutting the xenolith, are composed of phlogopite, potassian richterite, diopside, lindsleyite, and minor olivine, mathiasite, and corroded enstatite. Grains of chromian spinel are present in phlogopite and potassian richterite in veins and in the substrate.

This xenolith was among the first reported to contain lindsleyite and is unusual because it also contains a few grains of mathiasite (Haggerty et al., 1983). A more intensive optical study of the sample has been made using a new suite of polished sections and polished thin sections, carefully located to document the relationship between vein and substrate minerals. This study shows that a progressive transformation can be traced from lindsleyite in veins to a complex five-phase assemblage of chromian spinel, lindsleyite, hawthorneite, rutile, and ilmenite (Fig. 1a) in substrate material 1–2 cm away from veins, to unreacted chromian spinel at distances greater than 3–5 cm from veins. In most, but not all, cases, hawthorneite (50 × 100 μm in maximum dimension) is surrounded by a 10- to 20-μm veneer of lindsleyite separating chromian spinel from hawthorneite (Fig. 1b). The spinel is strongly corroded by embayments of hawthorneite and lindsleyite, with ilmenite and rutile (<<1 vol%) randomly disseminated as anhedral 10- to 15-μm grains.

OPTICAL AND PHYSICAL PROPERTIES

Hawthorneite is saturated in transition elements, is opaque, and, although identified only in polished section, is assumed to be black macroscopically with a metallic luster. In plane-polarized reflected light, in air, and in oil immersion, hawthorneite resembles lindsleyite and mathiasite but is much lighter gray relative to the coexisting magnesian chromite. It is free from internal reflections, nonpleochroic, and, depending on orientation, is weakly to moderately birefractant. It is also weakly to moderately anisotropic with brown and gray rotation tints and straight extinction.

Reflectance measurements were made relative to a SiC standard (Zeiss, no. 472), with Zeiss oil N_D 1.516 (at 20 °C), using the procedures outlined by Criddle in Cabri et al. (1981). Several randomly oriented grains were measured: the constancy of the R values for one vibration direction for all of these grains suggests that the mineral is uniaxial (negative). In Table 1, the R and mR data are for the most birefractant grain of hawthorneite (this grain was also analyzed; see analysis 1, Table 2), and R'_z and

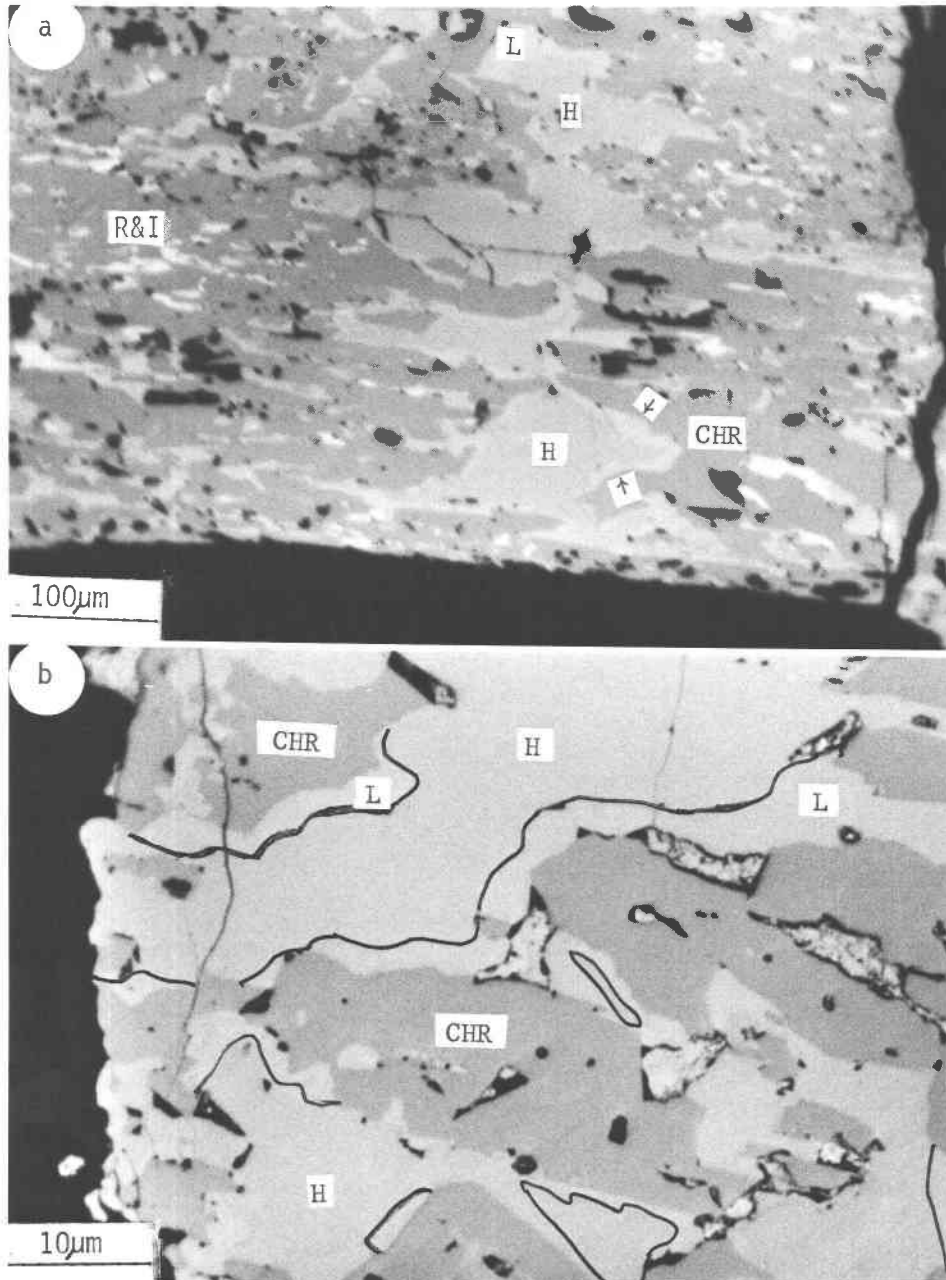


Fig. 1. (a) Replacement-textured magnesian chromian spinel (dark gray, CHR) infiltrated by the new mineral hawthorneite (H, medium gray). Hawthorneite is in direct contact with magnesian chromian spinel but is best illustrated in areas where it is surrounded by an annulus of lindsleyite (L) as shown by the arrows. The white stringers in the region of R and I, and else-

where, are niobian chromian rutile (R) and magnesian chromian ilmenite (I). (b) A higher-magnification photomicrograph illustrating the textural relationship between and among magnesian chromite (CHR), hawthorneite (H), and lindsleyite (L). Contacts between H and L are inked-in. Both photomicrographs are in reflected light and under oil-immersion objectives.

${}^{im}R'_e$, though probably not measured on the principal extraordinary vibration direction, are the nearest to R_e obtainable on randomly oriented sections. These data, and those for the least anisotropic and birefractant grain, are plotted in Figure 2. The reflectance values for hawthorneite are similar to those of lindsleyite and mathiasite (cf.

Stanley, in Haggerty et al., 1983), but hawthorneite may be distinguished from them by its greater birefractance and weaker dispersion.

The refractive indices calculated from the R and ${}^{im}R$ data at 590 nm, using Koenigsberger equations, are $n_o = 2.39$ and $n'_e = 2.33$; $r < v$ for the refringence and the

TABLE 1. Spectral reflectance data for hawthorneite

λ (nm)	R_o	R'_o	mR_o	${}^mR'_o$	λ (nm)	R_o	R'_o	mR_o	${}^mR'_o$
400	19.5	18.1	7.00	6.08	550	17.5	16.4	5.56	4.86
410	19.3	17.9	6.83	5.92	560	17.4	16.4	5.51	4.83
420	19.1	17.8	6.66	5.79	570	17.4	16.3	5.48	4.80
430	18.9	17.6	6.51	5.67	580	17.3	16.3	5.45	4.78
440	18.8	17.5	6.36	5.55	590	17.3	16.3	5.42	4.76
450	18.6	17.4	6.23	5.45	600	17.2	16.2	5.40	4.75
460	18.4	17.2	6.12	5.33	610	17.2	16.2	5.38	4.74
470	18.3	17.1	6.02	5.25	620	17.2	16.15	5.37	4.72
480	18.1	16.95	5.95	5.18	630	17.1	16.1	5.36	4.70
490	18.0	16.9	5.87	5.11	640	17.1	16.1	5.35	4.69
500	17.9	16.8	5.80	5.06	650	17.05	16.0	5.34	4.68
510	17.8	16.7	5.74	5.02	660	17.0	16.0	5.32	4.66
520	17.7	16.6	5.70	4.98	670	17.0	16.0	5.30	4.64
530	17.7	16.5	5.64	4.94	680	16.95	15.95	5.29	4.62
540	17.6	16.5	5.61	4.90	690	16.9	15.9	5.27	4.60
546	17.5	16.4	5.58	4.88	700	16.9	15.9	5.26	4.58

absorption. The reflectance data for yimengite (Dong et al., 1983) are very different from those of hawthorneite: as described, the mineral is gray to grayish white and weakly pleochroic; however, the reflectance data, if accurate, are for a mineral that is strongly blue-green pleochroic, strongly birefractant, and, it follows, strongly anisotropic. The inconsistency between what Dong et al. observed and measured throws some doubt on the validity of the optical data for yimengite.

Cross-sectional areas and total volumes of hawthorneite in polished section are extremely small. For this reason, only five micro-indentation hardness measurements were possible: $VHN_{100} = 772\text{--}835$, average of the five measurements = 801. The Mohs' hardness calculated from these figures is roughly 5.8. The indentation hardness of yimengite (Dong et al., 1983) is unusually low for a Ti- and Cr-bearing oxide at $VHN_{25} = 273$, equivalent to a Mohs' hardness of about 3.8 (Dong et al. calculated 4.1).

Neither cleavage nor parting planes are observed in hawthorneite, whereas in yimengite (Dong et al., 1983), cleavage along $\{0001\}$ is perfect with parting planes parallel to $\{10\bar{1}1\}$.

The calculated density of hawthorneite is 5.02 g/cm^3 , compared to 4.35 g/cm^3 for yimengite (Dong et al., 1983), 4.63 g/cm^3 for lindsleyite, and 4.60 g/cm^3 for mathiasite.

MINERAL CHEMISTRY

Electron-microbeam analyses of hawthorneite were performed in three laboratories [University of Massachusetts; CSIRO, Melbourne; and the British Museum (Natural History), London], on three instruments with different take-off angles (ETEC Autoprobe, Cameca Camebax, and Cambridge Microscan IX), and with three distinct sets of standards. Grains from three different polished sections (and/or polished thin sections) were used in the study, and the data for 27 analyses are summarized in Table 2. Among the major elements Ti, Cr, Fe, and Ba, the maximum variation is $\sim 3\text{ wt}\%$ as the oxide. Mg varies from 2.9 to 3.9 wt% MgO, and the minor elements Zr, Al, Mn, K, and Nb vary between 0.1 and 0.3 wt% as

oxides. Oxygen contents were determined on the Cameca at CSIRO, using an ODPB (stearate) analyzing crystal and benitoite as a standard, with internal checks on metals and oxide standards. The sample was coated with Al metal, which precluded analysis of Al; this was determined elsewhere to be a minor element in hawthorneite in the range of 0.2–0.5 wt% Al_2O_3 (Table 2).

Determination of oxygen contents has provided the most reliable estimates of Fe^{2+} and Fe^{3+} contents. Grey et al. (1987) have shown that hawthorneite has a magnetoplumbite-type structure, with a model chemical for-

TABLE 2. Compositions of hawthorneite and yimengite

	Hawthorneite				Yimengite	
	1	2	3	4	5	6
TiO ₂	25.84	23.31	22.94	22.20–23.60	29.15	30.75
ZrO ₂		0.13				
Al ₂ O ₃	0.48	0.23			1.61	1.30
Cr ₂ O ₃	31.00	31.46	34.05	33.04–34.85	37.06	36.94
FeO	23.22	24.84	13.83	23.25–24.86	18.36	17.80
Fe ₂ O ₃			11.31			
MgO	3.88	3.51	3.07	2.87–3.47	7.89	6.79
MnO	0.53	0.23	0.12	0.06–0.21	0.00	0.37
CaO		<0.01			0.00	0.20
BaO	13.13	13.63	12.52	12.01–13.04	1.61*	0.00
K ₂ O	0.36	0.45	0.55	0.54–0.58	3.75	3.92
Nb ₂ O ₅		0.26	0.16	0.09–0.33	0.00	0.18
Total	98.44	98.80	98.55†		99.98‡	98.56‡

Note: (1) British Museum (Natural History), London. Cambridge Microprobe. Standards: $MgCr_2O_4$, Al_2O_3 , KCl, TiO_2 , Mn, FeS, BaF_2 . Single analysis on grain used for reflectance measurements. (2) University of Massachusetts, Amherst. ETEC Autoprobe. Conditions and standards given in Haggerty et al. (1983). Average of 15 analyses. (3) CSIRO, Melbourne, Cameca Camebax. Standards: Benitoite, chromite, periclase, Mn-bearing ilmenite, ADU-compound for K, Nb. Average of 11 analyses. Oxygen determined and oxides are calculated. (4) Range of 11 analyses with average given in column 3. (5 and 6) Data from Dong et al. (1983). Column 5 is an average of two analyses and column 6 is an average of three analyses.

* BaO is not reported in the original publication, value given is from Zhou Jianxiang (written communication, 1984; personal communication to S.E.H., 1987).

† Also contains (wt%) SiO_2 0.06, Na_2O 0.10, La_2O_3 0.10, Ce_2O_3 0.31, and Ta_2O_5 0.18.

‡ Also contains SiO_2 of 0.55 and 0.31 wt% in analyses 5 and 6, respectively.

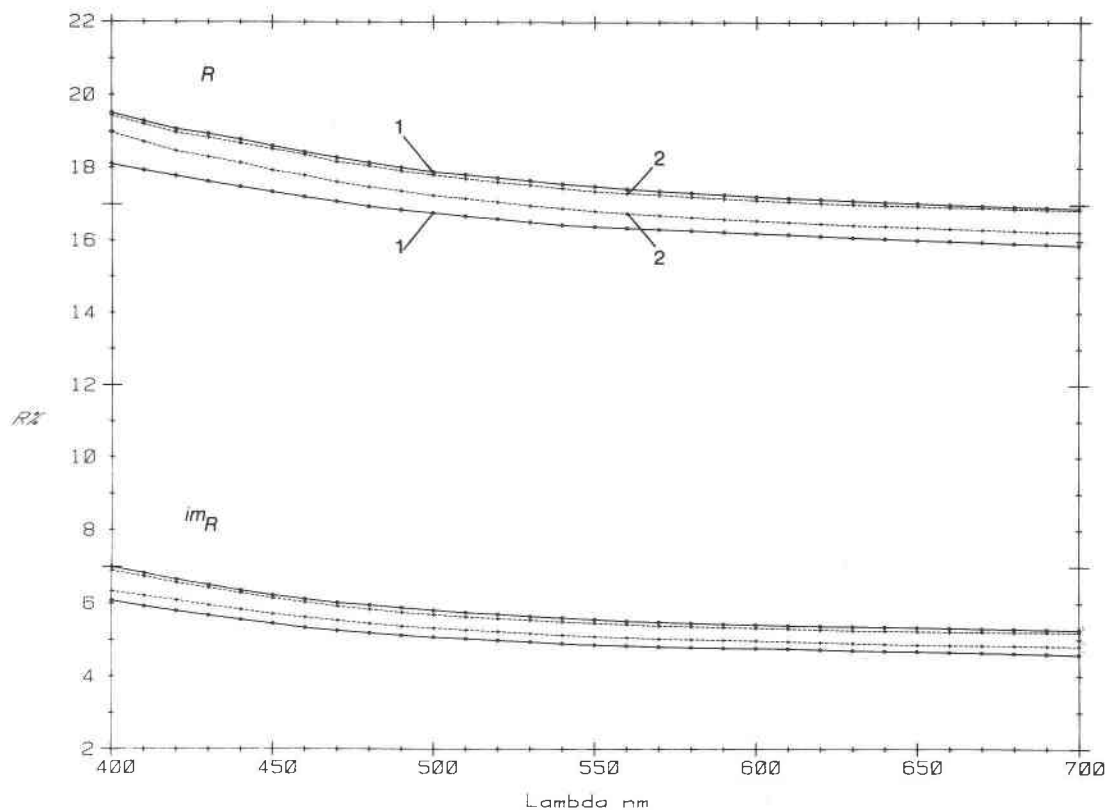
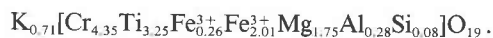


Fig. 2. The reflectance curves are for the most bireflectant (spectra 1) and least bireflectant (spectra 2) grains of hawthorneite.

mula of $\text{Am}_{12}\text{O}_{19}$, comparable to yimengite (Dong et al., 1983). The A site of hawthorneite is occupied by Ba with minor K, and in yimengite it is occupied by K with minor Ba. In assessing the $\text{Fe}^{2+}/\text{Fe}^{3+}$ ratio, therefore, the small M cation sites were normalized to 12 cations, and the calculation proceeded on the basis of 19 oxygens. The resulting formula for hawthorneite from Table 2, column 3, is



which, simplified, reduces to $\text{Ba}[\text{Cr}_4\text{Ti}_3\text{Fe}_4\text{Mg}]\text{O}_{19}$. A typical analysis for yimengite (Table 2, columns 5 and 6) yields



Apart from the difference in large cations, the only other significant difference is in the small-cation M sites, where Mg is more abundant by a factor of two in yimengite than in hawthorneite. Other oxides (Table 2) vary proportionately, with significantly higher concentrations of TiO_2 and Cr_2O_3 and lower contents of total Fe in yimengite relative to hawthorneite.

Compositions of other oxides intimately associated with

hawthorneite are given in Haggerty et al. (1986), where it is noted that the associated lindsleyite is depleted in ZrO_2 and enriched in TiO_2 relative to discrete crystals of lindsleyite in veins of the same specimen. Chromian spinel is enriched in TiO_2 (~8 wt%) with ~9 wt% MgO. Ilmenite is very unusual with large concentrations of Cr_2O_3 (9.5 wt% maximum) and moderately high MgO (~10 wt%). Rutile is also extraordinary with ~3 wt% Nb_2O_5 and 5–7 wt% Cr_2O_3 . For ilmenite and rutile, similar compositions are reported only in association with mathiasite from the Jagersfontein kimberlite, South Africa (Haggerty, 1983).

CRYSTALLOGRAPHY

A portion of the large composite grain shown in Figure 1 was excavated from the polished thin section and carefully fragmented and trimmed, following repeated analytical examination by SEM of the polished surface, in an attempt to obtain a single homogeneous grain of hawthorneite for single-crystal X-ray structural determination. Precession photographs of several fragments show spinel as the only attached mineral. Diffraction patterns display hexagonal symmetry and show that hawthorneite

TABLE 3. Calculated X-ray diffraction pattern of hawthorneite

<i>h</i>	<i>k</i>	<i>l</i>	<i>d</i> _{calc}	<i>I</i> _{calc}	<i>h</i>	<i>k</i>	<i>l</i>	<i>d</i> _{calc}	<i>I</i> _{calc}
0	0	2	11.530	1	1	1	10	1.813	4
0	0	4	5.765	<1	0	2	9	1.805	9
0	1	0	5.085	1	0	2	10	1.708	4
0	1	1	4.965	10	0	3	0	1.695	7
0	1	2	4.652	16	0	3	2	1.677	2
0	0	6	3.843	16	1	2	7	1.660	38
0	1	4	3.813	1	0	0	14	1.647	5
0	1	5	3.416	2	0	3	4	1.626	20
0	1	6	3.066	1	0	2	11	1.617	42
1	1	0	2.936	42	1	1	12	1.608	4
0	0	8	2.882	13	1	2	8	1.599	5
1	1	2	2.845	11	1	2	9	1.537	1
0	1	7	2.765	85	0	2	12	1.533	2
1	1	4	2.616	100	1	2	10	1.476	1
0	2	0	2.542	7	0	1	15	1.472	1
0	2	1	2.527	4	2	2	0	1.468	45
0	1	8	2.508	6	0	2	13	1.455	4
0	2	2	2.483	1	1	1	14	1.436	1
0	2	3	2.414	49	1	2	11	1.417	3
1	1	6	2.333	2	0	2	14	1.382	10
0	1	9	2.288	1	2	2	6	1.371	3
0	2	5	2.226	30	0	3	10	1.366	1
0	2	6	2.120	25	2	2	8	1.308	5
0	1	10	2.100	1	1	2	13	1.303	1
1	1	8	2.057	1	1	3	7	1.296	13
0	1	11	1.938	4	1	1	16	1.294	4
0	0	12	1.922	1	0	3	12	1.271	2
1	2	1	1.915	2					

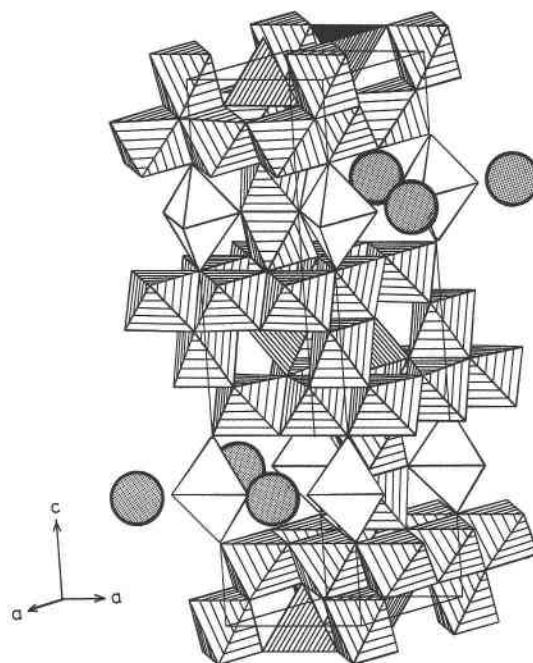


Fig. 3. Polyhedral representation of the structure of hawthorneite viewed approximately along [110]. Ba atoms shown by shaded circles. Unit-cell outline shown.

is isostructural with barium ferrite, $\text{BaFe}_{12}\text{O}_{19}$ (Townes et al., 1967), which has the magnetoplumbite structure (Adelsköld, 1938). Associated spinel has an orientation relationship to hawthorneite, with $[111]_{\text{sp}} \parallel [0001]_{\text{Haw}}$ and $(22\bar{4})_{\text{sp}} \parallel (30\bar{3}0)_{\text{Haw}}$.

With additional trimming, a crystal ($0.130 \times 0.088 \times 0.035$ mm) was selected and mounted for an intensity-data collection using a Siemens AED diffractometer and $\text{MoK}\alpha$ radiation. Structural details are given in Grey et al. (1987) with the following results: crystal-structure refinement to $R = 0.044$ was obtained for 368 independent reflections. Hawthorneite has hexagonal symmetry with space group $P6_3/mmc$ and cell parameters are $a = 5.871(2)$ Å, $c = 23.06(2)$ Å, $V = 688.33(7)$ Å³, and $Z = 2$. The structure is composed of slabs of a spinel-type structure, four anion layers thick, intergrown with perovskite-like BaO_3 close-packed layers parallel to $[111]_{\text{sp}}$. The Ba and Ti substitute, respectively, for tetrahedral Mg and octahedral Cr in magnesian chromian spinel. A representation of the structure, viewed approximately along [110], is shown in Figure 3.

A calculated X-ray diffraction pattern is given in Table 3. The three strongest reflections for hawthorneite are 2.616 Å (100), 2.765 Å (85), and 2.414 Å (49). By comparison, the dominant reflections in yimengite (Dong et al., 1983) are 2.608 Å (100), 2.753 Å (90), and 1.622 Å (90). Corresponding unit-cell dimensions for yimengite are $a = 5.8570(11)$ Å and $c = 22.9403(54)$ Å. Barium

ferrite, $\text{BaFe}_{12}\text{O}_{19}$, has $a = 5.8920(1)$ Å and $c = 23.183(1)$ Å (Obradors et al., 1985).

GENESIS

Veined harzburgitic xenoliths in kimberlites are characterized by hydrous minerals (phlogopite and potassian richterite), diopside, a suite of mineralogically unusual titanates (lindsleyite, mathiasite, yimengite, and now hawthorneite), and minor contents of armalcolite, rutile, and ilmenite (Erlank et al., 1987; Haggerty, 1987). Trace-element and isotopic studies (e.g., Erlank et al., 1987) show these harzburgites, previously depleted in major-element basaltic constituents, to be enormously enriched in LIL elements (such as Ba, K, Rb, and Sr) and in refractory silicate-incompatible elements (such as Ti, Zr, Nb, and LREE). Superimposed on this enriched signature are high concentrations of the restite elements Mg and Cr. All of this is unequivocally indicative of upper-mantle metasomatism and is unrelated to the sampling of xenoliths during kimberlite emplacement as shown by Sr-isotope studies (Erlank and Shimizu, 1977; Erlank et al., 1987).

The mineralogical gradient preserved in BD3096—from veinlet lindsleyite and rare mathiasite, to the complex five-phase assemblage of magnesian chromite, lindsleyite, hawthorneite, rutile, and ilmenite (Fig. 1a), to microscopically unaffected magnesian chromian spinel—is

interpreted as representing a geochemical metasomatic gradient in which a reaction has occurred between spinel and infiltrating fluid or melt. This reaction is confirmed by the oriented structural relationship of spinel and hawthorneite, by the textural relationship of lindsleyite and hawthorneite to spinel (Fig. 1b), and by the systematic decrease in Cr_2O_3 (48 wt% to 31 wt% to 12 wt%) and increase in TiO_2 (7 wt% to 23 wt% to 58 wt%) from magnesian chromian spinel to hawthorneite and lindsleyite. From the presence of potassian richterite and diopside, fluids or volatile-rich melts were enriched not only in Ba, Ti, Zr, and Nb but also in K, Na, and to a lesser extent Ca. Mg and Cr were largely derived from spinel to form the observed assemblage of large-cation barium titanates.

SUMMARY

The new mineral hawthorneite, $\text{Ba}[\text{Cr}_4\text{Ti}_3\text{Fe}_4\text{Mg}]_{19}\text{O}_{19}$, is opaque and has a magnetoplumbite-type structure with hexagonal symmetry. It is intimately intergrown with, and has a structural orientation to, magnesian chromian spinel. Hawthorneite also has a textural relationship to lindsleyite, and associated minerals are niobian chromian rutile and magnesian chromian ilmenite. Present in a reaction gradient related to veins of phlogopite, potassian richterite, and diopside, the new mineral and related assemblages offer an unusual opportunity to constrain the model behavior of elemental migration patterns at high P and T . Hawthorneite is interpreted to have formed by metasomatism in the upper mantle by reaction of fluids or fluid-rich melts with residual magnesian chromian spinel in geochemically depleted harzburgite. Hawthorneite ($\text{AM}_{12}\text{O}_{19}$) is an intermediate phase in the transformation of spinel to lindsleyite ($\text{AM}_{21}\text{O}_{38}$). Hawthorneite and associated minerals are estimated to have formed at depths of 75–100 km in the subcontinental lithosphere of the Kaapvaal craton (Haggerty, 1983), on the basis of the stability of lindsleyite (Podpora and Lindsley, 1984) and potassian richterite (Kushiro and Erlank, 1970).

Hawthorneite is the Ba analogue of yimengite, which is K-specific in the large-cation structural site (A) in magnetoplumbite isotypes. The latter are defined chemically as $\text{AM}_{12}\text{O}_{19}$, where M are small cations, dominated in these upper-mantle minerals by Ti, Cr, Mg, and Fe. Yimengites from the Shandong Province of China (Dong et al., 1983) and Venezuela (Nixon and Condliffe, 1989) are associated with chromian spinel and mathiasite (K-specific) and are considered to have formed in a similar manner to that of the association of chromian spinel, lindsleyite (Ba-specific), and hawthorneite (Ba-specific) from Bultfontein, South Africa. Possible differences are in fluid or melt activity and in large-cation, oxide-silicate partitioning coefficients.

The recognition of hawthorneite, in company with yimengite, lindsleyite, and mathiasite, broadens the spectrum of high-temperature and high-pressure oxide phases

in the upper mantle that are capable of hosting an exotic array of large-ion-lithophile and refractory, silicate-incompatible elements. It is becoming increasingly more important to incorporate these minerals into geochemical models, recognizing that the style and extent of upper-mantle metasomatism are remarkably similar and pervasive in widely separated subcontinental, subcratonic lithospheres.

ACKNOWLEDGMENTS

The sample used in this study was collected by J. Barry Dawson. Research was supported by the U.S. National Science Foundation (EAR86-06496), the Commonwealth Scientific and Industrial Research Organization, Australia, and the Foundation for Research and Development, South Africa. The manuscript was thoroughly reviewed by Roland C. Rouse. To all we express our appreciation.

REFERENCES CITED

- Adelsköld, V. (1938) X-ray studies on magneto-plumbite, $\text{PbO} \cdot 6\text{Fe}_2\text{O}_3$, and other substances resembling 'beta-alumina,' $\text{Na}_2\text{O} \cdot 11\text{Al}_2\text{O}_3$. *Arkiv för Kemi Mineralogi och Geologi*, series A-12, no. 29, 1–9.
- Cabri, L.J., Criddle, A.J., LaFlamme, J.H.G., Bearn, G.S., and Harris, D.C. (1981) Mineralogical study of complex Pt-Fe nuggets from Ethiopia. *Bulletin de Minéralogie*, 194, 508–525.
- Dong, Z., Zhou, J., Lu, Q., and Peng, Z. (1983) Yimengite ($\text{K}(\text{Cr}, \text{Ti}, \text{Fe}, \text{Mg})_{12}\text{O}_{19}$)—A new mineral. *Kexue Tongbao Bulletin Science*, 15, 932–936.
- Erlank, A.J., and Shimizu, N. (1977) Strontium and strontium isotope distributions in some kimberlite nodules and minerals. Extended Abstracts, 2nd International Kimberlite Conference, Santa Fe, New Mexico (unpaginated).
- Erlank, A.J., Waters, F.G., Hawkesworth, C.J., Haggerty, S.E., Allsopp, H., Rickard, R.S., and Menzies, M. (1987) Evidence for metasomatism in peridotite nodules from the Kimberley pipes, South Africa. In C.J. Hawkesworth and M. Menzies, Eds., *Mantle metasomatism*, p. 221–311. Academic Press, London.
- Gatehouse, B.M., Grey, I.E., Campbell, I.H., and Kelly, P. (1978) The crystal structure of loveringite—A new member of the crichtonite group. *American Mineralogist*, 63, 28–36.
- Grey, I.E., and Gatehouse, B.M. (1978) The crystal structure of landauite, $\text{Na}[\text{MnZn}_2(\text{Ti}, \text{Fe})_6\text{Ti}_2]\text{O}_{38}$. *Canadian Mineralogist*, 16, 63–68.
- Grey, I.E., and Lloyd, D.J. (1976) The crystal structure of senaite. *Acta Crystallographica*, B32, 1509–1513.
- Grey, I.E., Lloyd, D.J., and White, J.S. (1976) The structure of crichtonite and its relationship to senaite. *American Mineralogist*, 61, 1203–1212.
- Grey, I.E., Madsen, I.C., and Haggerty, S.E. (1987) Structure of a new upper-mantle magnetoplumbite-type phase $\text{Ba}[\text{Ti}_3\text{Cr}_4\text{Fe}_4\text{Mg}]_{19}\text{O}_{19}$. *American Mineralogist*, 72, 633–636.
- Haggerty, S.E. (1983) The mineral chemistry of new titanates from the Jagersfontein kimberlite, South Africa: Implications for metasomatism in the upper mantle. *Geochimica et Cosmochimica Acta*, 47, 1833–1854.
- (1987) Metasomatic mineral titanates in upper mantle xenoliths. In P.H. Nixon, Ed., *Mantle xenoliths*, p. 671–690. Wiley, Chichester, England.
- Haggerty, S.E., Smyth, J.R., Erlank, A.J., Rickard, R.S., and Danchin, R.V. (1983) Lindsleyite (Ba) and mathiasite (K): Two new chromium-titanates in the crichtonite series from the upper mantle. *American Mineralogist*, 68, 494–505.
- Haggerty, S.E., Erlank, A.J., and Grey, I. (1986) Metasomatic mineral titanate complexing in the upper mantle. *Nature*, 319, 761–763.
- Kushiro, I., and Erlank, A.J. (1970) Stability of potassic richterite. *Carnegie Institution of Washington Year Book* 68, 231–233.
- Nixon, P.H., and Condliffe, E. (1989) Yimengite of K-Ti metasomatic

- origin in kimberlitic rocks from Venezuela. *Mineralogical Magazine*, in press.
- Obradors, X., Collomb, A., Pernet, M., Samaras, D., and Joubert, J.C. (1985) X-ray analysis of the structural and dynamic properties of $\text{BaFe}_2\text{O}_{19}$ hexagonal ferrite at room temperatures. *Journal of Solid State Chemistry*, 56, 171–181.
- Podpora, C., and Lindsley, D.H. (1984) Lindsleyite and mathiasite synthesis of chromium-titanates in the crichtonite ($\text{AM}_{21}\text{O}_{38}$) series. *EOS*, 65, 293.
- Townes, W.D., Fang, J.H., and Perrotta, A.J. (1967) The crystal structure and refinement of ferrimagnetic barium ferrite, $\text{BaFe}_{12}\text{O}_{19}$. *Zeitschrift für Kristallographie*, 125, 437–449.
- Zhou, J., Yang, G., and Zhang, J. (1984) Mathiasite in kimberlite from China. *Acta Mineralogica Sinica*, 9, 193–200.

MANUSCRIPT RECEIVED AUGUST 15, 1988

MANUSCRIPT ACCEPTED JANUARY 3, 1989